Journal of Applied Electrochemistry **34**: 583–589, 2004.

Electrooxidation of aqueous *p*-methoxyphenol on lead oxide electrodes

C. BORRÁS*, P. RODRÍGUEZ, T. LAREDO, J. MOSTANY and B.R. SCHARIFKER
Departamento de Química, Universidad Simón Bolívar, Apartado 89000, Caracas 1080 A, Venezuela
*(*author for correspondence, fax: +58 212 906 3969, e-mail: cborras@usb.ve)*

Received 16 June 2003; accepted in revised form 3 December 2003

Key words: electrocatalysis, metal oxide anode, oxidation of organics, *p*-methoxyphenol

Abstract

Oxidation of *p*-methoxyphenol (pmp) in aqueous solution on bismuth-doped lead oxide was studied, and the effects of the initial pmp concentration, applied potential and hydrodynamic conditions upon the oxidation rate were identified. Under all conditions studied, the concentration decay of pmp during electrooxidation follows first–order reaction kinetics. Through analysis of rotating ring-disc currents, the faradaic efficiencies for oxidation at various concentrations of pmp in solution were determined. Using u.v.–vis. and H^1RMN spectroscopy for solution analysis, it is shown that partial oxidation of pmp occurs in chloride-free aqueous solutions. The principal products were *p*-benzoquinone and maleic acid, with low production of CO_2 up to 1000 C dm^{-3} charge. Mineralization to CO_2 was considerably improved upon addition of chloride ions to the solution. *In situ* FTIR spectra of the electrode surface during electrolysis indicated that the presence of chloride ions enhances the mineralization of pmp by reaction of benzoquinone with anodically generated hypochlorite.

1. Introduction

The electrochemical oxidation of phenol and substituted phenols on metal oxide electrodes has been studied for the direct degradation of contaminants in the treatment of residual waters [1–10]. It has been proposed [11–17] that the mechanism involves the adsorption of OH species produced from the oxidation of water molecules; these groups, or the oxides produced from electrochemical oxidation on the surface [18, 19], are the species that transfer oxygen to the organic compound during its oxidation.

Considering the participation of OH species, the reactions taking place on the electrode may be written as

$$M[\,] + H_2O \rightarrow M[OH] + H^+ + e^- \quad (1)$$

$$M[OH] + H_2O \rightarrow M[\,] + O_2 + 3H^+ + 3e^- \quad (2)$$

$$M[OH] + R \rightarrow M[\,] + RO + H^+ + e^- \quad (3)$$

where M[ ] corresponds to an adsorption site and R is the organic compound. Due to concurrent oxidation of water and the organic compound through pathways (1), (2) and (1), (3), evaluation of the electrocatalytic activity of the surface towards oxidation of the organic requires the distinct contributions of both processes to the total current to be determined.

In principle, phenols can be oxidized on classical anode materials. However, on such electrodes (C, Pt, Au) phenols cause anode inactivation by oligomer deposition on the surface [2, 6, 10, 14, 17, 20]. For this reason, metal oxide anodes (PbO_2, SnO_2, IrO_2) have been used to oxidize organic compounds in aqueous solution where the oxygen transfer reactions are fast [10, 12]. The performance of an anode material depends on the substance being oxidized. Thus the catalytic effect of PbO_2, SnO_2 and IrO_2 anodes observed during oxidation of chlorophenols changes with the number of chlorine atoms in the aromatic ring, and also with the position of these Cl atoms with respect to the phenolic OH [9, 10, 20].

It has been reported that the presence of chloride ions in solution enhances the mineralization of organic compounds [21, 22] through anodic generation of hypochlorite, which increases the oxidation rate of intermediates formed during their anodic oxidation. The results depend on the nature of the electrode used. For instance, a catalytic effect due to the presence of chloride has been observed during oxidation of phenol in chloride solutions onto Ti/IrO_2, but such an effect was not observed on Ti/SnO_2 [22].

Here we present a study of the oxidation of *p*-methoxyphenol (pmp) in aqueous solution on bismuth-doped lead(IV) oxide electrodes, carried out to explore the effects of different parameters, electrode potential, initial concentration of pmp and mass transport conditions, on the kinetics of oxidation of pmp. The aim is to establish the reaction mechanism as well as the efficiency of the process for generation of CO_2. For this purpose,

u.v.–vis. and FTIR spectroscopy was used to follow the composition of the solution during electrolysis at constant potential, as a function of the electric charge passed through the electrode|solution interface. Since Cl^- is usually present in wastewater, we also studied the effect of its presence on pmp degradation; the results show that the rate of oxidation of intermediates is increased in the presence of Cl^-, leading to higher efficiencies for CO_2 generation.

2. Experimental details

Rotating ring-disc experiments were carried out with a Pine Instruments bipotentiostat (model AFMSR) and gold–platinum ring-disc electrode, under Pinechem v.2.73 software. A three-compartment glass cell was used throughout, in order to maintain the solution in the working electrode compartment separated from that contacting the 2.2 cm^2 platinum wire used as secondary electrode, as well as that in contact with the saturated calomel electrode (SCE) used as reference. All potentials are reported with respect to the SCE unless otherwise stated. Reagents were of analytical grade (Aldrich or Sigma) and water used for preparation of all solutions was first distilled and then ultrafiltered (Nanopure).

PbO_2 + Bi_2O_3 was deposited onto the gold disc from a 1 mM Pb^{2+} + 0.1 mM Bi^{3+} + 1 M $HClO_4$ solution at 1.6 V constant potential for 30 min, as described by Johnson [23]. The bare gold surface was recovered when necessary by dissolving the deposit in 1 M $HClO_4$ at 0.2 V, followed by polishing with 0.3 μm alumina. Oxidation of pmp was studied in aqueous 0.01 M solution in the presence of 0.1 M Na_2SO_4.

The collection efficiency, N, of the ring-disc electrode was determined from a plot of the current at the ring, I_R, as a function of the current at the disc, I_D, obtained in potassium hexacyanoferrate(II) solution, maintaining the ring at −0.32 V and varying the disc potential. N was found to be 0.22.

Extensive electrolyses were carried out at 1.65 V vs SCE using an EG&G (PAR model 273) potentiostat, using PbO_2–Bi covered platinum gauze with larger geometrical surface area as working electrode. In these experiments the working electrode compartment was filled with 20 ml of phenol-containing solution, vigorously stirred with a magnetic stirrer during electrolysis.

The variation of pmp concentration during electrolysis at 1.65 V vs SCE was determined from u.v.–vis. spectra. Spectroscopic data were obtained with a Hewlett-Packard 8452A diode-array spectrometer under HP 89531 MS-DOS u.v.–vis. Operating Software, from 100 μl aliquots sampled from the electrolysis cell at different times, and diluted to 10 ml with water. The experimental u.v.–vis. spectra thus obtained were deconvoluted into Lorentzian bands with Jandel Peakfit v. 3.0. The concentrations of the different compounds present in solution were determined using the Lambert–Beer law, with the molar absorption coefficients ε obtained from literature data at the wavelengths of maximum absorption for each compound, as indicated in Table 1.

Table 1. Wavelengths of maximum absorption and molar absorption coefficients of analysed compounds

Compound	λ /nm	$10^{-3}\ \varepsilon$ /cm^{-1} M^{-1}	Ref.
p-methoxyphenol (pmp)	288	6.8	24
p-benzoquinone (pbq)	248	19.7	25
maleic acid (ma)	210	13.8	26

After electrolysis at constant potential, the solutions changed colour from light-yellow to reddish-brown, with formation of a precipitate, which was centrifuged from solution and then dissolved in CD_3Cl, and later analysed using a 400 MHz Jeol Eclipse + pulsed-NMR spectrometer.

A 1 cm diameter gold disc covered with PbO_2–Bi was used for i.r. spectroelectrochemical measurements. The syringe-type all-glass cell used and other experimental details have been previously described [27]. *In situ* subtractively normalized interfacial Fourier transform infrared spectra were obtained with an Equinox IFS-55 (Bruker) spectrometer, with a medium band (MIR, 700–6000 cm^{-1}) globar source and a liquid nitrogen-cooled MCT detector by Fourier transformation after averaging 300 interferograms at 4 cm^{-1} resolution using *p*-polarized radiation, and expressed in $\Delta R/R_0$ units. $\Delta R = R - R_0$, where R is the reflected i.r. signal at the applied potential, and R_0 is the reference signal acquired at 0.9 V vs SCE.

3. Results and discussion

3.1. *U.v.–vis. analysis*

Figure 1 shows u.v.–vis. spectra obtained during electrolysis of an aqueous pmp solution on the bismuth-

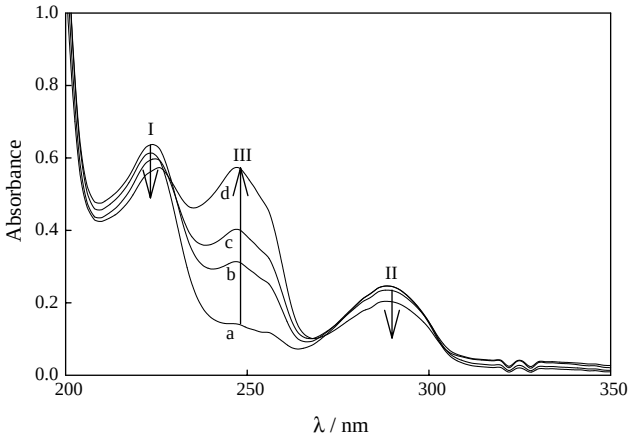

Fig. 1. U.v.–vis. spectra of 0.01 M *p*-methoxyphenol (pmp) + 0.1 M Na_2SO_4 aqueous solution, during electrolysis on PbO_2–Bi rotating disc electrode at $\omega = 209$ rad s^{-1} and 1.65 V, during (a) 0, (b) 7.5, (c) 18 and (d) 30 C dm^{-3}.

doped lead oxide electrode at 1.65 V. The 210–240 nm (I) and 265–310 nm (II) bands observed in the spectrum obtained at the onset of the electrolysis are associated to pmp. The band at 230–265 nm (III) rises as pmp is degraded during electrolysis giving way to isosbestic points at around 225 and 265 nm. The appearance of colouration in the solution and the position of band III in the spectrum, suggest the formation of a quinoid compound during electrolysis. A precipitate was observed in electrolysed solutions after standing overnight. The ^{1}HNMR spectra of the centrifuged solid in CD_3Cl showed signals at chemical shifts of 6.78 and 6.70 ppm, consistent with the formation of quinhydrone arising from the presence of 1,4 benzoquinone in the electrolysed solution.

The oxidation kinetics may be determined from the concentration decay of pmp during electrolysis, dc_{pmp}/dt, which may be determined from the diminishing intensity of bands I and II in Figure 1. However, due to the proximity and overlap of the bands in the u.v.–vis. spectra, the variation of concentration of pmp was determined by adding 4-aminoantipyrine to the electrolysed samples [28], after which a single band due to pmp appears between 450 and 600 nm, thus avoiding overlap with the band of the oxidation product. The decay of absorbance due to the presence of pmp, dA_{pmp}/dt, determined from this method matches the increasing intensity of band III in Figure 1; therefore both criteria may be used to follow the kinetics of the reaction in its initial stages.

3.2. *Influence of electrode potential*

The rate of formation of benzoquinone in solution depends on the electrode potential, as shown in Figure 2. The rate increases with potential up to a constant value at potentials beyond 1.65 V vs SCE, corresponding to an anodic current of about 2.5 mA. Even though the anodic current continues increasing as the potential becomes more positive, the rate of formation of benzoquinone remains practically invariant; thus the increase in the anodic current is mainly due to the increasing rate of oxygen evolution (Reaction 1), with the net result of a decrease in the faradaic efficiency for pmp oxidation. The constant rate of formation of benzoquinone observed at potentials more positive to 1.65 V was found to be consistent with the $4e^-$ limiting current for pmp oxidation to benzoquinone, predicted from the Levich equation. From this result we chose 1.65 V as the potential for pmp oxidation under the conditions of the present work.

3.3. *Influence of the initial concentration of pmp*

It has been shown [29, 30] that from the currents measured at the ring, the ring-disc electrode allows discrimination of the contributions of the different processes occurring during oxidation of organic compounds at metal oxide disc electrodes. The disc current I_D is the sum of contributions due to oxidation of the organic compound, I_{pmp} in our present case, and formation of molecular oxygen, I_O:

$$I_D = I_{pmp} + I_O \tag{4}$$

I_O may be determined from the oxygen reduction current at the ring and then I_{pmp} may be determined by subtracting I_O from the disc current. This may be expressed as:

$$I_{pmp} = I_D - I_O = I_D + I_R/N \tag{5}$$

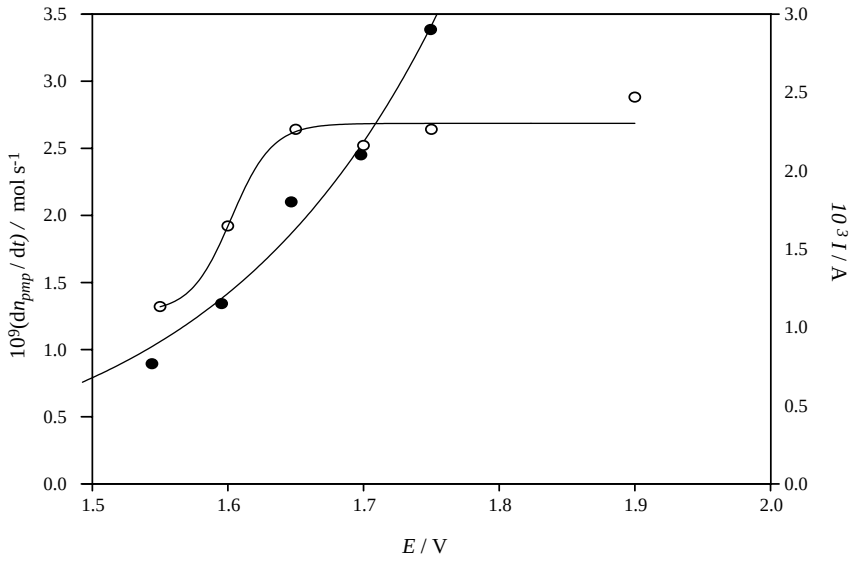

Fig. 2. pmp oxidation rate (○) and current (●) on PbO_2–Bi rotating disc electrode at $\omega = 209$ rad s^{-1} in 0.01 M pmp + 0.1 M Na_2SO_4 aqueous solution, as a function of the applied potential.

where N is the collection efficiency of the ring-disc electrode, defining the fraction of the amount of species generated at the disc that are collected at the ring.

The faradaic efficiency of pmp oxidation is given by the relation:

$$\gamma = I_{\mathrm{pmp}}/I_{\mathrm{D}} \tag{6}$$

Figure 3 shows the faradaic efficiency as a function of the initial concentration of pmp. The faradaic efficiency for pmp oxidation first rises as pmp successfully competes with water for the oxidation sites, but then at higher concentrations the rate of pmp oxidation, and hence γ, becomes essentially independent of pmp concentration. This is frequently observed in processes requiring the co-adsorption of reactants, as described by the Langmuir–Hinselwood model [31].

3.4. *Mass transport*

Figure 4 shows the rate of oxidation of pmp as a function of the square root of the angular rotation rate of the electrode, $\omega^{1/2}$. Each of the measurements was carried out on freshly prepared Bi–PbO_2 films and solutions. The oxidation rate increases with the rotation rate; however, the linear dependence between oxidation rate and $\omega^{1/2}$ predicted by the Levich equation [32] does not hold at high rotation rates, suggesting that the rate of the process is controlled by slow reaction kinetics at large mass transfer rates.

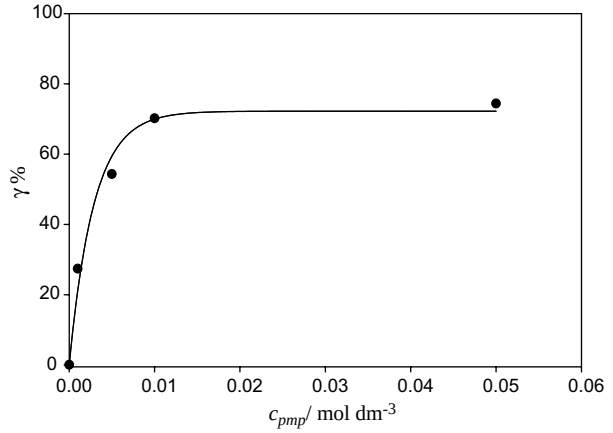

Fig. 3. Initial faradaic efficiency of pmp oxidation on PbO_2–Bi rotating disc electrode at $\omega = 209$ rad s^{-1} as a function of initial concentration of pmp in 0.1 M Na_2SO_4 aqueous solutions.

3.5. *Kinetic constant*

The kinetic constant can be obtained considering that the degradation reaction follows first order kinetics

$$\mathrm{d}c_{\mathrm{pmp}}/c_{\mathrm{pmp}} = k_{\mathrm{app}}\mathrm{d}t \tag{7}$$

where c_{pmp} is the concentration of pmp at time t and k_{app} is the apparent rate constant. The integral form of Equation 7 is

$$-\ln[c_{\mathrm{pmp}}]_{\mathrm{t}}/c_{\mathrm{pmp},0} = k_{\mathrm{app}}t \tag{8}$$

where $c_{\mathrm{pmp},0}$ is the initial concentration of pmp. Figure 5 shows the linear plots of $\ln [c_{\mathrm{pmp}}]_{\mathrm{t}}/c_{\mathrm{pmp},0}$ with t obtained, from which the slope k_{app} was obtained as 6×10^{-4} s^{-1}. The decaying pmp concentration due to the heterogeneous reaction may be represented as

$$-\mathrm{d}c_{\mathrm{pmp}}/\mathrm{d}t = kN_0\theta_{\mathrm{OH}}\Gamma_{\mathrm{pmp}} \tag{9}$$

where k is the heterogeneous rate constant, N_0 represents the surface density of adsorption sites (cm^{-2}), θ_{OH} is the fractional surface coverage by OH_{ads} arising from the discharge of water, and Γ_{pmp} is the surface concentration of pmp. k was found from k_{app} as $k = k_{\mathrm{app}}V/A$, where V is the solution volume, 20 cm^3, and A is the real area of the electrode, 2×10^2 cm^2, as obtained from analysis of adsorption isotherms [33] for a roughness factor of 1×10^3. The heterogeneous rate constant k was thus found to be $k = 6 \times 10^{-5}$ cm s^{-1}.

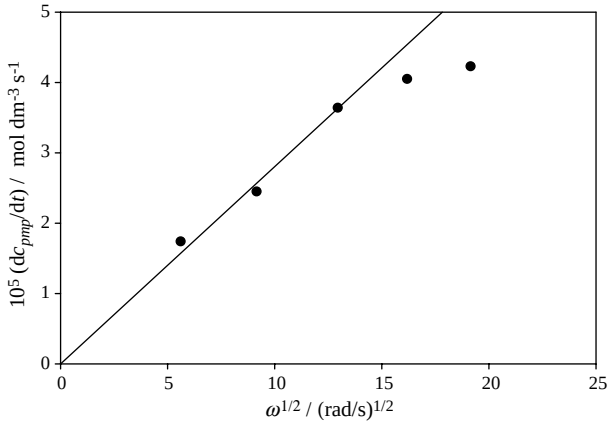

Fig. 4. Oxidation rate ($\mathrm{d}c/\mathrm{d}t$) of pmp on PbO_2–Bi rotating disc electrode from 0.01 M pmp + 0.1 M Na_2SO_4 aqueous solution as a function of the square root of rotation rate ($\omega^{1/2}$) at 1.65 V vs SCE.

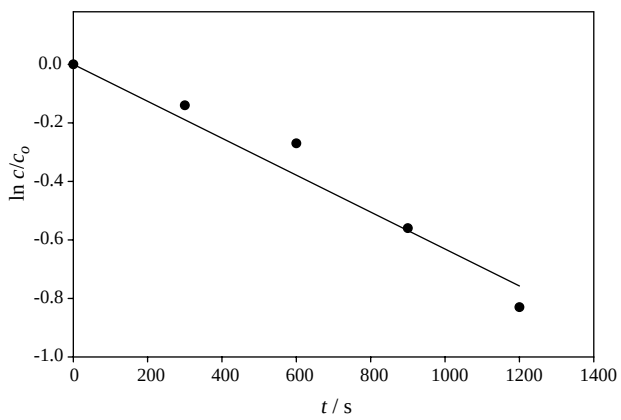

Fig. 5. Linear regression for pmp disappearance rate with time during electrochemical oxidation of 0.01 M pmp in solution on PbO_2–Bi rotating disc electrode at $\omega = 209$ rad s^{-1} and 1.65 V.

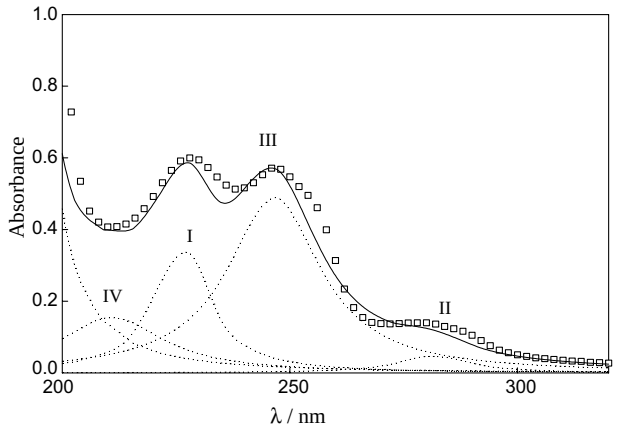

Fig. 6. U.v.–vis. spectrum of 0.01 M pmp + 0.1 M Na_2SO_4 solution, after electrolysis under stirring at 1.65 V vs SCE on PbO_2–Bi covered Pt gauze, and the passage of 1200 C dm^{-3} electric charge; (□ □ □) experimental, (——) deconvoluted spectrum.

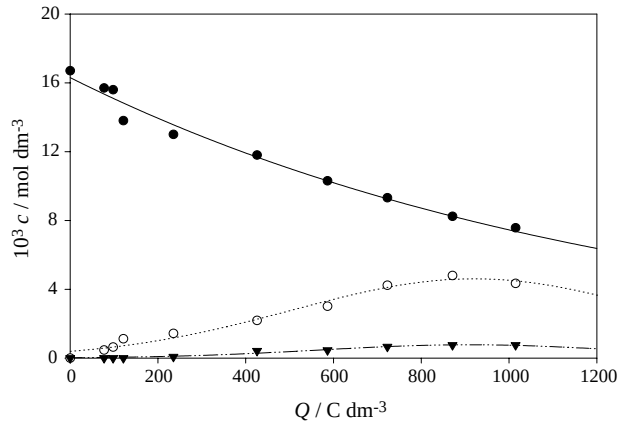

Fig. 7. Intensity of absorption bands in 0.01 M pmp + 0.1 M Na_2SO_4 solution, as a function of the electric charge passed during electrolysis under stirring at 1.65 V vs SCE on PbO_2–Bi covered Pt gauze. Band I, $\lambda = 288$ nm, pmp (●); band III, $\lambda = 248$ nm, *p*-benzoquinone (○); band IV, $\lambda = 210$ nm, maleic acid (▼).

3.6. *Electrolyses*

The kinetics of oxidation at long times was followed with u.v.–vis. spectra. Figure 6 shows the deconvoluted spectrum obtained after passing 1200 C dm^{-3} of electric charge at 1.65 V vs SCE through 0.01 M pmp and 0.1 M Na_2SO_4 aqueous solution. While bands I and II associated to pmp decrease with electrolysis time, band III of bq increases. A fourth band, band IV, appeared in the spectra obtained after passing a certain amount of charge. This fourth band is associated to the presence of aliphatic acids (maleic acid, ma) in solution [1, 4, 12, 20]. Superposition of bands and their variation in opposite directions as electrolysis progressed hampered the resolution of the kinetics of oxidation directly from the spectra; however, this could be readily circumvented by following the change in intensity of bands after deconvolution of the spectra into their component bands as discussed above.

Figure 7 shows the concentration of the principal products formed in solution with the electric charge (C dm^{-3}) during electrolysis at 1.65 V vs SCE. The bq concentration increased up to a maximum at about 900 C dm^{-3}. For charge values higher than 400 C dm^{-3} the ma was present in solution in low concentration. From these results the reaction mechanism may be represented as

$$R_1 \xrightarrow{k_1} R_2 \xrightarrow{k_2} R_3 \xrightarrow{k_3} R_4 \tag{10}$$

where $R_1 =$ pmp, $R_2 =$ bq, $R_3 =$ ma and $R_4 = CO_2$. The increase in concentration of bq in solution observed experimentally and the delay for the appearance of ma indicate that oxidation of pmp is faster than oxidation of bq.

3.7. *Influence of chloride ions*

The rates of consumption of pmp and formation of ma obtained from deconvoluted spectra of solutions during electrolysis at different Cl^- concentrations are shown in Figure 8. Although the presence of chloride enhances mineralization through the anodic generation of hypo-

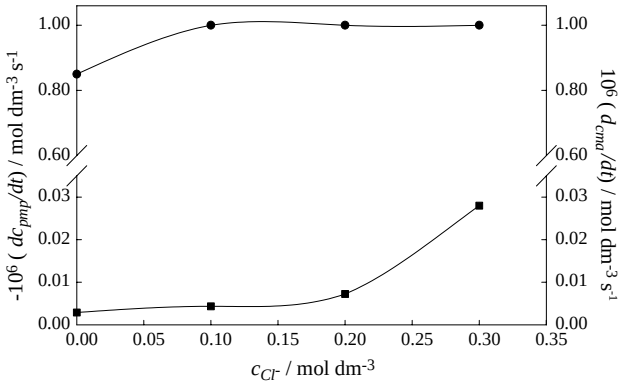

Fig. 8. Decay rate of pmp (●) and formation rate of maleic acid (■) during electrolysis at 1.65 V vs SCE on PbO_2–Bi covered Pt gauze under stirring, in 0.01 M pmp + 0.1 M Na_2SO_4 solution + *x* M NaCl, as a function of the concentration of chloride ions in solution.

chlorite [21, 22], the results indicate that the presence of Cl^- in solution does not lead to significant increase in the rate of consumption of pmp when compared to 0.1 M Na_2SO_4 solutions in the absence of Cl^-. However, the rate of formation of ma increases with Cl^- concentration for concentrations higher than 0.15 M. It was also observed that, upon increasing the Cl^- concentration, the yellowish-brown colour of the solution, characteristic of the presence of quinoid species, vanished. As stated above, the slow step in Equation 10 is the oxidation of benzoquinone (bq). Once formed bq dissolves into solution losing interaction with surface OH; the increased rate of formation of ma indicates that reaction of bq occurs in solution, with a species formed from the anodic oxidation of Cl^-. Furthermore, the invariance of the rate of oxidation of pmp with Cl^- concentration suggests that hypochlorite produced from chloride oxidation is not sufficiently oxidizing so as to directly oxidize pmp in solution; pmp oxidation occurs instead on the electrode surface, through adsorbed intermediates with surface concentrations not depending on the chloride ion concentration. u.v.–vis. spectra of 0.01 M pmp in aqueous 5% sodium hypochlorite solution showed no decay of pmp concentration even after 30 min of sampling, providing further support for this assertion.

Since pmp and the intermediates involved in its mineralization, bq and ma, are accounted for in the u.v.–vis. intensities obtained from the spectra, the fraction of pmp converted to CO_2 may be obtained from the spectral response and is given by the relation,

$$f_{CO_2} = 1 - (c_{pmp} + c_{bq} + c_{ma})/c_{pmp,0} \quad (11)$$

where c_{pmp}, c_{bq} and c_{ma} are the concentrations of pmp, bq and ma at any time of electrolysis, and $c_{pmp,0}$ is the initial concentration of pmp. Figure 9 shows the fraction of pmp converted to CO_2 as a function of the charge passed through the electrode–solution interface, both in the presence and absence of chloride ions. In solutions without Cl^-, CO_2 generation accounted for only about 10% of $c_{pmp,0}$ even after passing large charges. Since bq was the main product found, this confirms that ring opening is the rate determining step [12]. However, in the presence of 0.3 M Cl^-, CO_2 production increased to 34% of $c_{pmp,0}$ but remained virtually constant with the charge passed, indicating accumulation of ma in solution by oxidation of bq. This implies that only bq is oxidized by the hypochlorite electrogenerated from anodic oxidation of Cl^-.

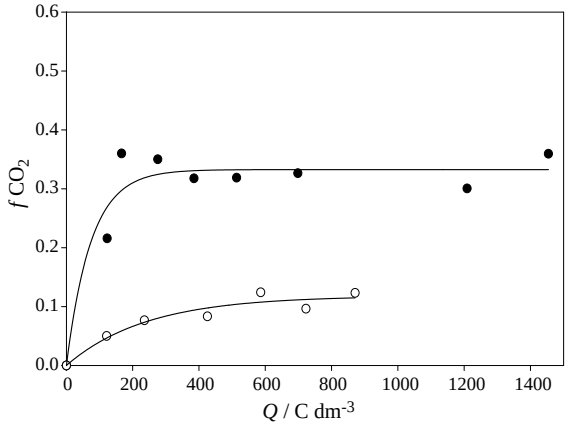

Fig. 9. Fraction of pmp converted to CO_2 (f_{CO_2}) as a function of the electric charge passed during electrolysis at 1.6 V vs SCE on PbO_2–Bi covered Pt gauze under stirring, in 0.01 M pmp + 0.1 M Na_2SO_4 (○) and 0.01 M pmp + 0.3 M NaCl. (●).

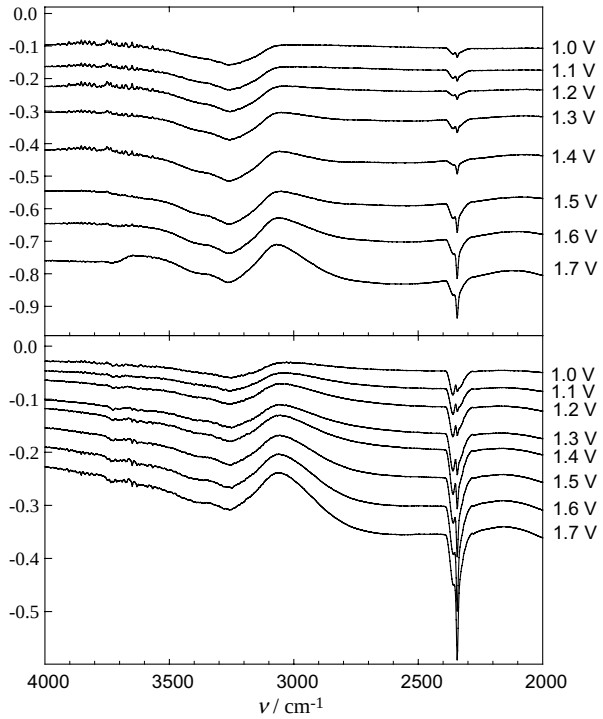

Fig. 10. In situ subtractively normalized interfacial Fourier transform infrared spectra of PbO_2–Bi in 0.01 M pmp + 0.1 M Na_2SO_4 (a) and 0.01 M pmp + 0.1 M NaCl (b) aqueous solution at the potentials indicated. Reference spectra were obtained at 0.9 V vs SCE.

Figure 10 shows *p*-polarized SNIFTIRS spectra of PbO_2–Bi electrodes in 0.01 M pmp solution in the absence (Figure 10(a)) and in the presence (Figure 10(b)) of chloride ions, between 1.1 and 1.7 V vs SCE at 0.1 V intervals. Figure 10(a) shows a wide band around 3250 cm^{-1} due to OH stretch, associated to the solvent, and a signal at 2320 cm^{-1} due to CO_2 dissolved in solution, produced from mineralization of pmp, with increasing intensity as the applied potential is made more positive. Performing a similar experiment in the presence of 0.1 M Cl^- (Figure 10(b)) shows the 2320 peak with much higher intensity, thus demonstrating enhancement in the mineralization of the compound. Due to interference from the wide bands in the region between 1800 and 1000 cm^{-1} associated to the solvent and SO_4^{2-} supporting electrolyte, it proved not possible to identify from the SNIFTIR spectra the signals due to pmp or reaction intermediates.

4. Conclusions

The oxidation rate of pmp on PbO_2–Bi was found to increase with applied potential, attaining a limiting rate at sufficiently positive potentials. Since the rate of oxygen evolution increases continuously with potential, at a certain point the current efficiency for pmp oxidation decreases as the potential increases. In chloride-free solutions, the current efficiency is constant for concentrations of pmp higher than 0.01 mol dm^{-3}. Under these conditions partial oxidation of pmp occurs, as confirmed using u.v.–vis. and H^1RMN spectroscopy for the product analysis obtained during electrolysis, where the principal products found in solution were *p*-benzoquinone (bq) and maleic acid (ma). CO_2 production was low in the interval of charge between 0 and 1000 C dm^{-3}. In chloride-containing solutions, on the other hand, mineralization to CO_2 in similarly treated samples was considerably enhanced. Hypochlorite resulting from oxidation of Cl^- [30] readily oxidizes benzoquinone to maleic acid, thus preventing accumulation of benzoquinone in solution. The oxidation of maleic acid to CO_2 then appears to be the rate-determining step for the mineralization of pmp in the presence of Cl^-.

Acknowledgements

We are grateful to Universidad Simón Bolívar and FONACIT for financial support, Michele Milo for managerial and technical assistance, the members of the Electrochemistry Group at USB for discussions, and Professor Julio Herrera from the Fitochemistry Laboratory of Universidad Simón Bolívar.

References

1. H. Sharifian and D.W. Kirk, *J. Electrochem. Soc.* **133** (1986) 921.
2. M. Gattrell and D.W. Kirk, *J. Electrochem. Soc.* **140** (1993) 1534.
3. B.J. Hwang and K.L. Lee, *J. Appl. Electrochem.* **26** (1996) 153.
4. N.B. Tahar and A. Savall, *J. Appl. Electrochem.* **29** (1999) 277.
5. Ch. Comninellis and C. Pulgarin, *J. Appl. Electrochem.* **23** (1993) 108.
6. M. Gattrell and D.W. Kirk, *J. Electrochem. Soc.* **140** (1993) 903.
7. D.C. Johnson, J. Feng and L.L.Houk, *Electrochim. Acta* **46** (2000) 323.
8. A.M. Polcaro, S. Palmas, F. Renoldi and M. Mascia, *Electrochim. Acta* **46** (2000) 389.
9. A.M. Polcaro, S. Palmas, F. Renoldi and M. Mascia, *J. Appl. Electrochem.* **29** (1999) 147.
10. J.D. Roogers, W. Jedral and N.J. Bunce, *Environ. Sci. Technol.* **33** (1999) 1453.
11. B. Fleszar and J. Ploszynska, *Electrochim. Acta* **30** (1985) 31.
12. N.B. Tahar and A. Savall, *J. Electrochem. Soc.* **145** (1998) 3427.
13. J.E. Vitt and D.C. Johnson, *J. Electrochem. Soc.* **139** (1992) 774.
14. K. Jüttner, U. Galla and H. Schmieder, *Electrochim. Acta* **45** (2000) 2575.
15. C. Bock and B. MacDougall, *J. Electroanal. Chem.* **491** (2000) 48.
16. L. Gherardini, P.A. Michaud and M. Panizza, Ch. Comninellis and N. Vatistas, *J. Electrochem. Soc.* **148** (2001) D78.
17. Ch. Comninellis and C. Pulgarin, *J. Appl. Electrochem.* **21** (1991) 703.
18. O. Simond ,V. Schaller and Ch. Comninellis, *Electrochim. Acta* **42** (1997) 2009.
19. G. Foti, D. Gandini. Ch. Comninellis, A. Perret and W. Haenni, *Electrochem. Solid State Lett.* **2** (1999) 228.
20. M.S. Ureta-Zañartu, P. Bustos, M.C. Diez, M.L. Mora and C. Gutierrez, *Electrochim. Acta* **46** (2001) 2545.
21. F. Bonfatti, A. De Battisti, S. Ferro, G. Lodi and S. Osti, *Electrochim. Acta* **46** (2000) 305.
22. Ch. Comninellis and A. Nerini, *J. Appl. Electrochem.* **25** (1995) 23.
23. W.L. LaCourse, Y. Hsiao and D.C. Johnson. *J. Electrochem. Soc.* **136** (1989) 3714.
24. 'The Sadtler Handbook of Ultraviolet Spectra', Sadtler Research Laboratories (1979).
25. J.W. Robinson, 'Handbook of Spectroscopy', Vol. II (CRC Press, OH, 1974).
26. E.A. Braude, *J. Chem. Soc.* **45** (1945) 490.
27. I. Rodríguez, B.R. Scharifker and J. Mostany, *J. Electroanal. Chem.* **491** (2000) 117.
28. L. Clesceri, 'Métodos Normalizados para el Análisis de Aguas Potables y Residuales' (Diaz de Santos, Madrid, 1989), p. 556.
29. N.D. Popovic and D.C. Johnson, *Anal. Chem.* **70** (1998) 468.
30. Y. Hu, Y.V. Tolmachev and D.A. Scherson, *J. Electroanal. Chem.* **468** (1999) 64.
31. I.Ilisz, Z. Laszlo and A. Dombi, *Applied Catálisis A*: *General* **180** (1999) 25.
32. A.J. Bard and L.R. Faulkner, 'Electrochemical methods: Fundamentals and Applications' (John Wiley & Sons, New York, 2nd edn, 2001).
33. C. Borras, T. Laredo and B.R. Scharifker, *Electrochim. Acta* **48** (2003) 2775.